Research article

SURFACE and INTERFACE ANALYSIS

Received: 9 June 2016 Revised: 16 August 2016 Accepted: 18 September 2016 Published online in Wiley Online Library: 6 October 2016

(wileyonlinelibrary.com) DOI 10.1002/sia.6183

Surface-interface microstructures and binding strength of cathodic arc ion plated TiCN coatings on YT14 cutting tools

Sun Ze,[a] Kong Dejun[a,b]* and Liu Wei[a]

A titanium carbonitride (TiCN) coating was deposited on YT14 cutting tool by using a CAIP (cathodic arc ion plating). The surface-interface morphologies, chemical compositions, and phases of TiCN coatings were observed by using a FESEM (field emission scanning electron microscopy), EDS (energy dispersive spectroscopy), XRD (X-ray diffraction), respectively, and the bonding energy, surface roughness, and bonding strength were characterized with an XPS (X-ray photoelectron spectroscopy), AFM (atomic force microscope), and scratch test, respectively. The results show that the phases of the TiCN coating are primarily composed of TiN, TiC, and amorphous C, of which the TiC and TiN increases the coating hardness, and the amorphous C atom improves friction and lubrication properties of the coating. The effect of CAIP on the topography of the TiCN coating is at nano-scale, the Ti and N atoms are enriched in the coating at the bonding interface, and the part of chemical elements are diffused in the gradual transformation layer. The bonding form of the TiCN coating interface is primarily composed of mechanical combination, accompanying with slight metallurgical combination, and the bonding strength is characterized with 60.85 N by scratch test. Copyright © 2016 John Wiley & Sons, Ltd.

Keywords: CAIP (cathodic arc ion plating); TiCN coating; surface and interface; plane scan; line scan; bonding strength

Introduction

Titanium carbonitride (TiCN) coating with high hardness, superior chemical, and thermal stability is a solid solution of TiN and TiC, which has a combine wear-resistant characteristic of both TiN and TiC.[1] It is widely applied in industry to improve the wear resistance of cutting tool[2] and has been already paid much attention in modern industry field.[3] As compared with TiN and TiC coatings, the TiCN coatings with the excellences of TiC and TiN possess lower COF (coefficient of friction) and higher wear resistance.[4] Therefore, the fabrications of TiCN coatings become a research focus at China and aboard, researchers focused on the fabrication of TiC or TiN coatings separately in the previous studies, and several works are reported. Bonding strength of the coating-substrate is a critical importance for the coating performance, and many researches have been made to investigate for a way to improve the cohesion and adhesion properties.[5] Cathodic arc ion plating (CAIP) is the most attractive due to the high ionization rate, high ion energy, and high deposition rate, and high bonding strength,[6] which is one of the most popular physical vapor deposition (PVD) techniques used on the industrial production of hard coatings,[7] improving bonding strength of the coatings. However, up to now, there are only a few reports on cathodic arc ion planting TiCN coating. In this study, a TiCN coatings were deposited on YT14 cutting tool by using a CAIP, the surface-interface morphologies, distributions of chemical elements, and phases of the TiCN coating were analyzed with a field emission scanning electron microscopy, energy dispersive spectroscopy (EDS), and X-ray diffraction (XRD), respectively, and the bonding energy, surface roughness, and bonding strength were characterized with an X-ray photoelectron spectroscopy (XPS), atomic force microscope (AFM), and scratch test, respectively, which provided a scientific base for application of TiCN coating on surface modification treatment of cutting tools.

Experimental

The substrate material was YT14 cutting tool with the chemical compositions as follows (mass, %): WC 78, TiC 14, and Co 8. The samples were polished with 80#–2000# sandpapers in turn, and polished to mirror with diamond grinding paste. Before being put into the vacuum chamber, the samples were cleaned with pure acetone using ultrasonic oscillation for 10 min and dried for the deposition in a PVT coating system. To deposit TiCN coatings, the industrial high purity C_2H_2 and N_2 were used as the working gas. The Ti with the purity of 99.99% was used as the target, and the deposition parameters were showed as follows: vacuum of 3×10^{-3} Pa, deposition temperature of 500 °C, and deposition time of 60 min. After annealing at 180 °C for 2 h, the coating samples were cleaned with acetone on a KQ2200DE type CNC ultrasonic cleaner, then cleaned with ultrasonic deionized water, and dried

* Correspondence to: Kong Dejun, School of Mechanical Engineering, Changzhou University, Changzhou 213164, China.
E-mail: kong-dejun@163.com

a School of Mechanical Engineering, Changzhou University, Changzhou 213164, China

b Jiangsu Key Laboratory of Materials Surface Science and Technology, Changzhou University, Changzhou 213164, China

SURFACE and INTERFACE ANALYSIS

with a hairdryer; the required samples were obtained. The morphologies, plane scan, and line scan of the TiCN coating-interface were observed with a JSUPRA55 type field emission scanning electron microscopy and its configured EDS, respectively, and the phases of the coating were analyzed with a D/max2500PC type XRD. The bonding energy of chemical elements in the coating was analyzed with a Thermo ESCALAB 250 type XPS, the test parameters: excitation source of X-ray: monochrome Ka Al (hv = 1486.6 eV), power of 150 W, beam spot of X-ray: 500 μm, fixed transmission energy of energy analyzer: 30 eV. The surface roughness and grain sizes of TiCN were researched with a CSPM5500 type AFM, of which the resolution can reach anometer level. The bonding strength of the coating was measured quantitatively with a WS-2005 type film adhesion automatic scratch tester, and the measurement method was acoustic emission, and the scratch parameters: load of 100 N, loading rate of 50 N/min, and scratch length of 6 mm.

Analysis and discussion of results

Surface morphology and plane scans

The TiCN coating surface contained about 1 μm aggregated particles, and the plane scanned position of the TiCN coating surface was shown in Fig. 1a, the result of plane scans was shown in Fig. 1b, the mass fractions of chemical elements were shown as follows: Ti 49.98, C 17.44, N 21.24, O 11.35; and the corresponding atomic fractions were Ti 22.10, C 30.75, N 32.12, O 15.03. The EDS mapping was carried out on the coating, which had Ti, C, and N as major components on the surface. The plane scans of Ti (Fig. 1c), C (Fig. 1d), and N (Fig. 1e) show that the Ti, C, and Ti elements were uniformly distributed on the coating surface, and the aggregations of chemical elements appeared on the similar positions.

X-ray photoelectron spectroscopy analysis

Figure 2 shows the high-resolution Ti2p, N1s, C1s, and O1s XPS spectra from the TiCN coatings, which were the typical

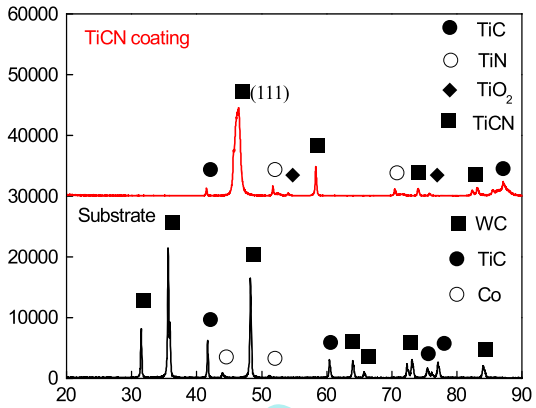

Figure 2. X-ray photoelectron spectroscopy full spectrum of titanium carbonitride coating surface. [Colour figure can be viewed at wileyonlinelibrary.com]

deconvolution results. The coating was primarily composed of Ti, C, and N elements; in addition, there was a contaminant of O element, which came from O element adhering to the sample surface as exposing in the air.

The peaks of Ti2p were at a binding energy of 458.29 and 463.15 eV, which was corresponded to the Ti-N bond of 2p3/2 and the TiC bond of 2p1/2,[6,8] as shown in Fig. 3a. The XPS spectrum of N1s exhibited a slightly symmetric peak at the binding energy of 399.78 eV, as shown in Fig. 3b, indicating that most of the N atoms in the coating were bonded to the Ti atoms. The peak spectra of C1s were at the binding energy of 284.78 eV, shown in Fig. 3c, which was assigned to the C-C bond originated from the adventitious carbon, there existed a large amount of amorphous carbon in the TiCN coatings during the CAIP, indicating that most of the C atoms existed as amorphous C. The high fraction absorbed amorphous C in the coatings explained the high-defect density in the TiCN coatings.[6] During the wear, the kind of C atom would form a transmission film, which decreased friction force and shearing force between the contacted surfaces, playing a role of dry

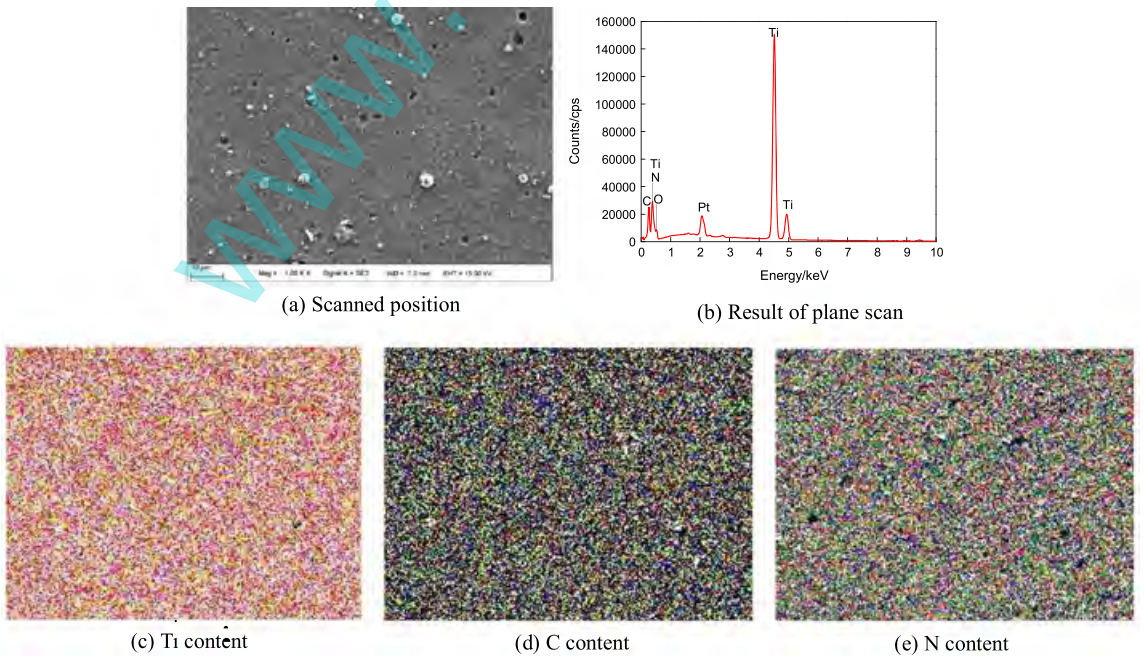

(a) Scanned position

(b) Result of plane scan

(c) Ti content

(d) C content

(e) N content

Figure 1. Plane scans of titanium carbonitride coating surface. [Colour figure can be viewed at wileyonlinelibrary.com]

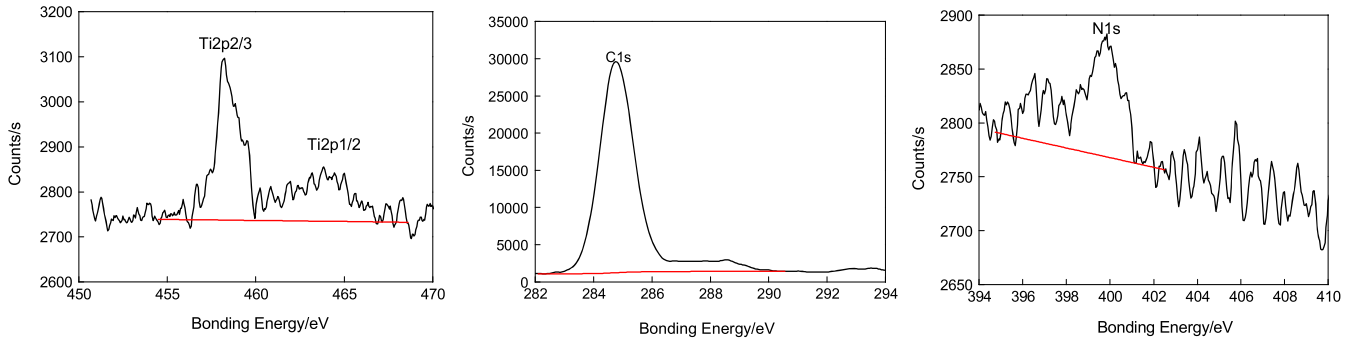

Figure 3. High-resolution X-ray photoelectron spectroscopy spectra of Ti2p, N1s, and C1s. [Colour figure can be viewed at wileyonlinelibrary.com]

lubricant. Therefore, the TiCN coating had anti-friction performance, which improved wear resistance of the coating.

X-ray diffraction analysis

Figure 4 shows the XRD analysis results of the YT14 cutting tool and the TiCN coating. The diffraction peaks of WC, TiC and Co were detected in the substrate, which were the compositions of YT14 cutting tool sintered by the hard phases of WC, TiC, and the binder of Co. The diffraction peaks of TiCN, TiN, TiC, and TiO_2 were detected in the coating, which was composed of Ti, N, and C elements, besides containing a small number of O atoms, which was consistent with the EDS analysis result in Fig. 3c and the XPS analysis result in Fig. 2. The C existed in the forms of amorphous C and TiC, the N existed in the form of TiN, and the Ti existed in the form of TiN and TiC. The formation of TiCN was that the N position of TiN was partly replaced by C atoms to form a substitutional solid solution structure with FCC (face centered cubic) of δ-NaCl, and the C atoms entered into the TiN lattices at a solid solution way, producing an elastic strain field. The C atoms were the center of the elastic strain field, when the dislocation movement appeared near the C atoms, and the larger resistance force was produced, increasing microhardness of the TiCN coatings.[9,10] Because the lattice constant of TiN was slightly smaller than that of TiC coating, the lattice constant of TiCN coating was between TiN and TiC coatings. The TiCN coating had a strong preferential growth along the direction of crystal face (111), this was because that the crystal face (111) was the dense face, and the TiCN coating was preferentially grew at the direction of crystal face (111), which had a significant effect on the increasing of the coating microhardness.

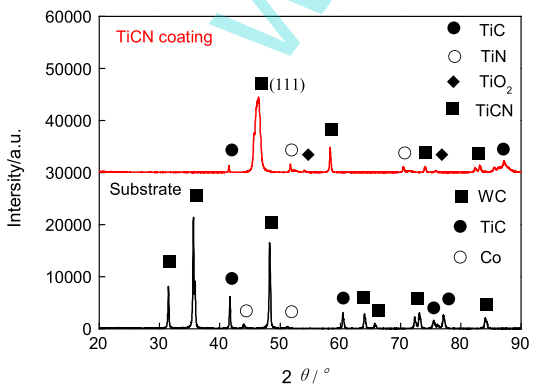

Figure 4. X-ray diffraction analysis of titanium carbonitride coatings and substrate. [Colour figure can be viewed at wileyonlinelibrary.com]

Atomic force microscope analysis

Atomic force microscope was carried out to quantitatively research the surface topography of TiCN coatings deposited on the YT14 cutting tool. Figure 4 shows AFM images of the substrate and TiCN coating with statistical distribution of grain sizes that were analyzed by the area of 90000 nm × 90000 nm. From Fig. 5, it can be seen as follows: (i) the S_a (outline arithmetic average deviation) of the substrate was 0.00557 nm while that of the coating was 0.00966 nm, about 1.73 times of the S_a of the substrate, this was because that ion bombardment generated some microscopic pits and convex peaks during the CAIP.[11,12] (ii) The S_q (root mean square value of roughness deviation from the reference benchmark) on the substrate was 0.0141 nm while that on the coating was 0.0128 nm, which was closed to the S_q on the substrate, showing that the topography undulating of the coating surface was small. (ii) The S_{sk} (tolerance of surface windage relative to the reference surface symmetry) on the substrate was −11.1 while that on the coating was 0.747, which was greater than zero, indicating that there were some convex peaks above the datum plane of the coating. (iv) The S_{ku} (shape height distribution) on the substrate was 382 while that on the coating was 5.48, showing that the coating surface topography was closed to Gaussian surface with the S_{ku} of 5. (v) The S_y (maximum height of the outline) on the substrate was 1 nm, while that on the coating was 0.2 nm, indicating that the S_y on the coating was superior to that on the substrate. (vi) The S_z (average height of five highest peaks and depth of 5 deepest pits) on the substrate was 0.935 nm, while that on the coating was 0.174 nm, showing that the coating surface was more relatively smooth.

In the measured area, the total number of grain on the coating and the substrate was 2217, and 7528, respectively. The corresponding average diameter was 866.2 and 1536 nm, respectively, and the average height was 0.01889 and 0.02226 nm, respectively, as shown in Fig. 6.

Interface morphology and plane scans

The coating thickness was about 1.75 μm, as shown in Fig. 7. The TiCN coating with a finer microstructure on YT14 cutting tool was dense, homogeneous, and featureless. This was a contribution to the microhardness, which was probably due to the addition of C element.[13] The coating exhibited a more gradual transformation

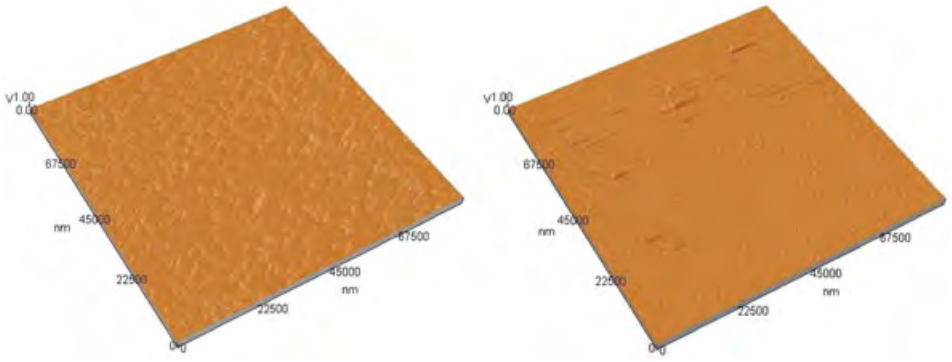

Figure 5. Atomic force microscope images of titanium carbonitride coating and substrate. [Colour figure can be viewed at wileyonlinelibrary.com]

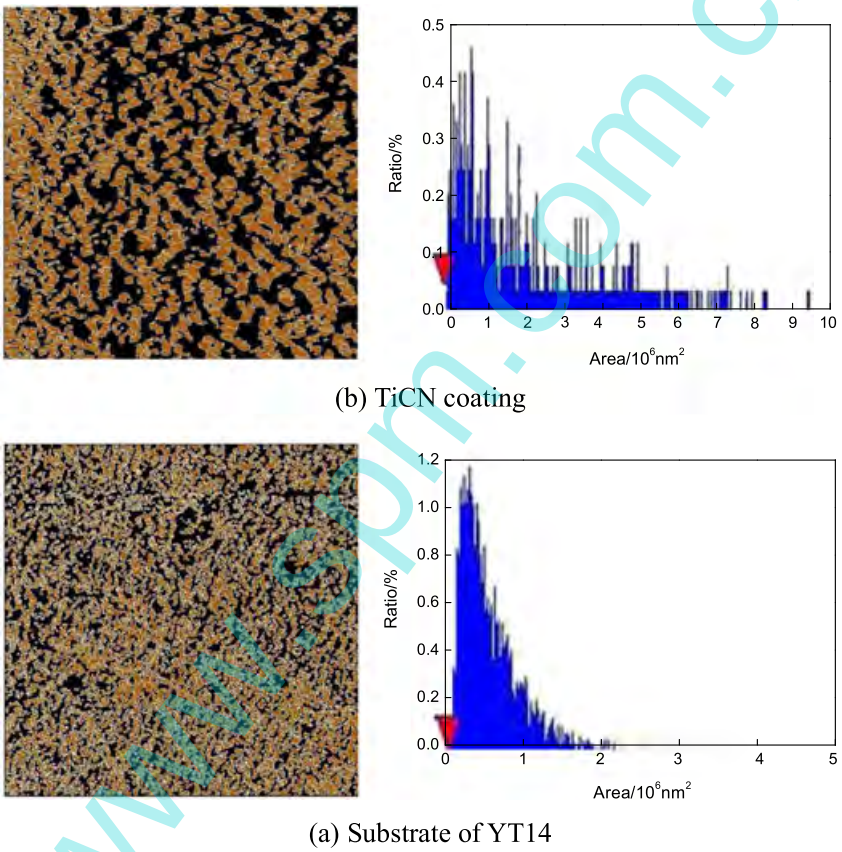

Figure 6. Particle size and proportion analysis of the substrate and coating. [Colour figure can be viewed at wileyonlinelibrary.com]

in the compositions between the coating and the substrate occurred over a length scale (~1 μm). The effect of CAIP was better observed in the cross-sectional micrographs, in which low-total porosity together with several grain boundaries were distinguished. The element distributions were confirmed by the chemical mapping images of the same area of Fig. 7a, the Ti atoms were located in the red colored areas (Fig. 7b, showing that the high concentrations of Ti atoms were enriched in the coating. Because of that there was the high concentrations of C atoms in the substrate, the C concentration in the coating-substrate were no obvious, shown as in Fig. 7c. The N atoms were also located in the blue colored areas (Fig. 7d), showing that the high concentrations of N atoms were enriched in the coating. Furthermore, the W, Co, Ni, Cr, and Fe atoms also recorded (Fig. 7 e–h), which were enriched in the YT14 cutting tool.

Line scans of interface

The line scan result shows in Fig. 8, the coating maintained the high concentrations of Ti, C, and N, and the substrate had the constant W and Ti without N. There was a compositionally graded layer between the coating-substrate, showing the gradual decreases of Ti, C, and N and the corresponding increases of W in the direction of the coating-substrate. This graded layer was formed, probably because a small amount of N_2 gas remained even after the gas flow stopped.[14] The free C was relatively concentrated in the coating,

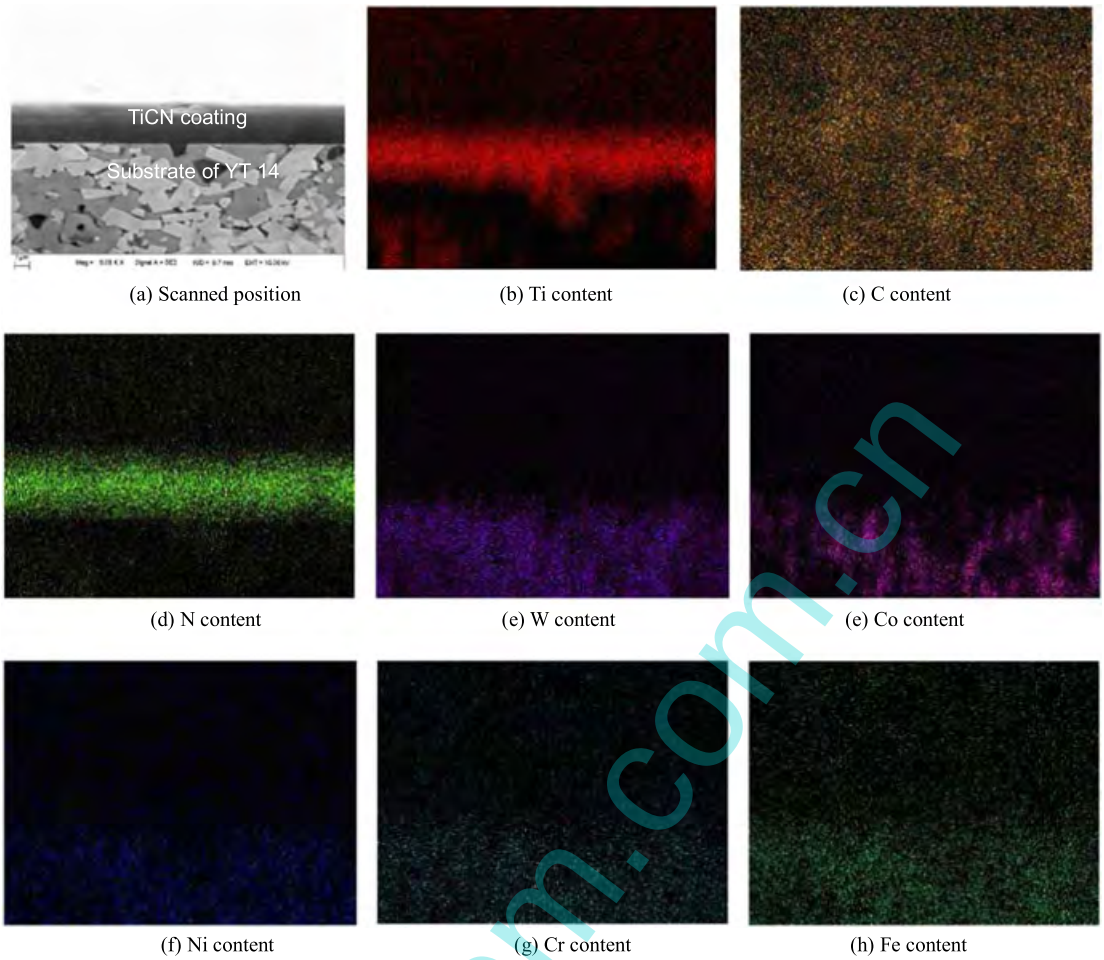

Figure 7. Plane scans of titanium carbonitride coating interface. [Colour figure can be viewed at wileyonlinelibrary.com]

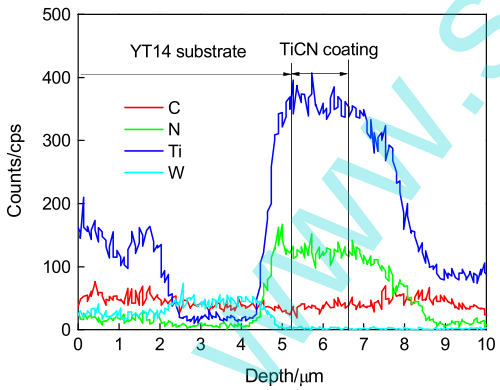

Figure 8. Line scans of titanium carbonitride coating interface. [Colour figure can be viewed at wileyonlinelibrary.com]

because N_2 gas tended to remove free C,[15] as explained the aforementioned analyses. In addition, the O element was not detected throughout the layer, showing that the presence of O element came from the pollutions on the coating surface.

Interfacial bonding strength

Figure 9a shows the scratch morphologies of the TiCN coating, the failure modes in scratch test, and acoustic emission; fluctuation versus normal load for the tested coatings was markedly different. As the diamond stylus was sliding with increasing normal load on the coating surface, the coating followed the deformation of the YT14 substrate,[16] which was divided into three stages: elastic stage, plastic stage, and failure stage. The tensile stress both inside the coating and at the interface led to cracking and delamination of the coatings. The acoustic emission signal was observed at a load of $L_c = 60.85$ N, as shown in Fig. 9b, which was bonding strength of the coating. The scratch test results matched well with the observation from the scratch in Fig. 9a, showing the scratch tracks of the TiCN coating on the YT14 substrate with increasing loads from 0 to 100 N. During the CAIP, ion bombardment with high energy activated the atoms on the substrate surface, and the diffusion and displacement was produced metallurgical bonding at the interface, improving the coating density,[17] so the coating presented higher bonding strength.

Figure 10 (a) shows the scratch morphology, which was a semicircular crack within the range of scratch scar. The stretched cracks were parallel with the diamond indenter of the scratch, and the density had an increasing trend with the scratch processing. The scratched surface in Fig. 10a was analyzed with a plane scan, the concentrations of Ti, C, and N in the coating shown a decrease phenomenon at the scratch edge of coating surface in Fig. 10b–d. While the concentration of W in the substrate shown an increase phenomenon in Fig. 10e, indicating that the white area in Fig. 10b was the substrate surface, at the time, the coating surface had failed and spelled from the substrate.

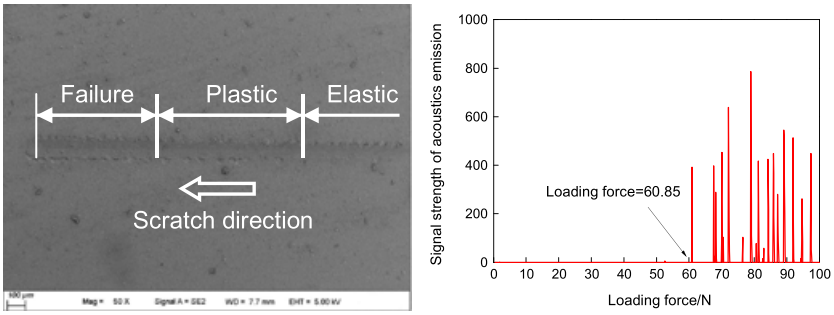

(a) Scratch morphology (b) Bonding strength

Figure 9. Scratch morphology and bonding strength of titanium carbonitride coating. [Colour figure can be viewed at wileyonlinelibrary.com]

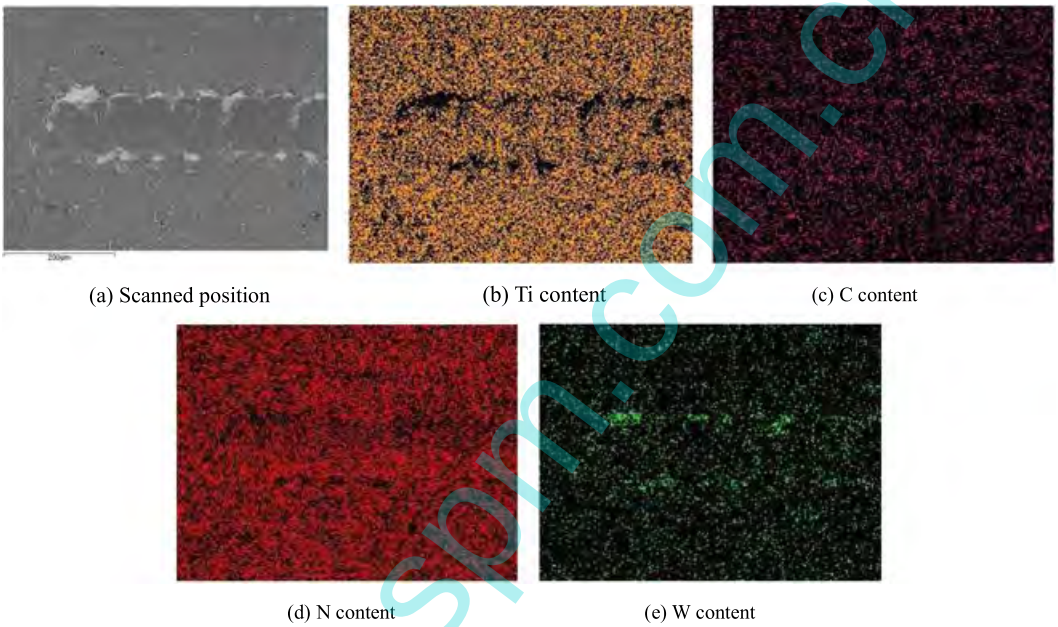

(a) Scanned position (b) Ti content (c) C content

(d) N content (e) W content

Figure 10. Plane scans of scratch zone. [Colour figure can be viewed at wileyonlinelibrary.com]

Conclusions

(1) The cathodic arc ion plated TiCN coating is primarily composed of Ti, C, and N elements, of which the Ti and N atoms form Ti-N bond, most of the C atoms exist as amorphous C, and only a few of the C and Ti atoms form Ti-C.
(2) The AFM analyses show that the effect of CAIP on the topography of the TiCN coating is at nano-scale.
(3) The thickness of the TiCN coating is about 1.75 μm, the Ti and N atoms are enriched in the coating, and the part of chemical elements in the coating and substrate is diffused at the gradual transformation layer.
(4) The compositionally graded layer is formed at the TiCN coating-substrate interface, showing high-bonding strength, which is characterized with 60.85 N by scratch test.

Acknowledgements

Financial support of this research by the Jiangsu Province Science and Technology Support Program (Industry) (BE2014818) is gratefully acknowledged.

References

[1] R. J. Talib, A. M. Zaharah, M. A. Selamat, *Procedia Eng*, **2013**, *68*, 716–722.
[2] T. Wolfgang, M. Soroush, *J Phy Chem Solids*, **2016**, *90*, 45–53.
[3] Q. Z. Wang, F. Zhou, S. Gao, Z. F. Zhou, L. K. Y. Li, J. W. Yan, *Wear*, **2015**, *328–329*, 356–362.
[4] Z. Y. Zeng, H. Q. Xiao, X. H. Jie, Y. M. Zhang, *Trans Nonferrous Met Soc China*, **2015**, *25*(11), 3716–3722.
[5] V. Sáenz de Viteri, M. G. Barandika, U. Ruiz de Gopegui, R. Bayón, C. Zubizarreta, X. Fernández, A. Igartua, F. Agullo-Rueda, *J Inorg Biochem*, **2012**, *117*, 359–366.
[6] M. D. Bao, X. B. Xu, H. J. Zhang, X. P. Liu, L. H. Tian, Z. X. Zeng, Y. B. Song, *Thin Solid Films*, **2011**, *520*(2), 833–836.
[7] L. Escobar-Alarcon, V. Medina, E. Camps, S. Romero, M. Fernandez, D. Solis-Casados, *Appl Surf Sci*, **2011**, *257*(21), 9033–9037.
[8] L. Zhang, G. J. Ma, H. Ma, G. Q. Lin, *Nucl Instr Meth Phys Res*, **2014**, *333*, 1–5.
[9] I. Zukerman, A. Raveh, H. Kalman, J. E. Klemberg-Sapieha, L. Martinu, *Wear*, **2007**, *263*(7–12), 1249–1252.
[10] S. Louring, N. D. Madsen, M. Sillassen, A. N. Berthelsen, B. H. Christensen, K. P. Almtoft, H. Ronkainen, L. P. Nielsen, J. Bøttiger, *Surf Coat Technol*, **2014**, *245*, 40–48.
[11] D. J. Kong, G. Z. Fu, *J Mater Res*, **2015**, *30*(4), 503–511.
[12] S. L. Ma, K. W. Xu, W. Q. Jie, *Surf Coat Technol*, **2005**, *191*, 201–205.

[13] D. J. Kong, G. Z. Fu, *Sci China Technol Sci*, **2015**, *58*(1), 1360–1368.
[14] P. G. Allison, C. A. Weissjr, R. D. Moser, A. J. Diaz, O. G. Rivera, S. S. Holton, *Compos Part B Eng*, **2015**, *78*, 131–137.
[15] S. Shimada, M. Takahashi, H. Kiyono, J. Tsujino, *Thin Solid Films*, **2008**, *516*, 6616–6621.
[16] C. T. Wang, A. Escudeiro, T. Polcar, A. Cavaleiro, R. J. K. Wood, N. Gao, T. G. Langdon, *Wear*, **2013**, *306*, 304–310.
[17] D. J. Kong, H. Y. Guo, *Int J Adv Manuf Technol*, **2016**, *85*, 2597–2605.